The Effects of CO$_2$ Pressure on Corrosion and Carburization Behaviors of Chromia-forming Austenitic Alloys

Ho Jung Lee, Sung Hwan Kim, Changheui Jang *
Dept. of Nuclear and Quantum Engineering, KAIST, Daejeon, Rep. of Korea
Corresponding author: chjang@kaist.ac.kr

1. Introduction

A supercritical-carbon dioxide (S-CO$_2$) Brayton cycle has been considered as one of the promising energy conversion systems in sodium-cooled fast reactor (SFR) [1]. By applying S-CO$_2$ cycle to SFR, the inherent safety could be improved by alleviating the concern of explosive reaction between high temperature steam and liquid sodium as well as increased thermal efficiency at 500-550 ºC compared to helium Brayton cycle.

Meanwhile, from the material point of view, a compatibility such as corrosion and carburization of candidate materials in S-CO$_2$ environment should be evaluated to assure the long-term integrity of IHX. It has been previously reported that Ni-base alloys and high-Cr Fe-base austenitic alloys showed a good corrosion resistance by the formation of thin chromia layer while carburization behaviors of those materials were not properly investigated [2-4].

Therefore, in this study chromia-forming austenitic alloys were exposed to different CO$_2$ pressures (S-CO$_2$ condition of 200 bar and atmospheric pressure of 1 bar). By comparing the effects of CO$_2$ pressure on corrosion and carburization behaviors, the mechanism of those phenomena in S-CO$_2$ environment will be discussed.

2. Methods and Results

2.1 Materials and Experimental

Three commercial grade chromia-forming austenitic alloys (Alloy 600, Alloy 690, and Alloy 800HT) were used in the test. The chemical compositions are listed in Table 1. For the corrosion tests, the test materials were machined to coupon type specimens (12 mm in diameter and 1 mm in thickness) and ground to 1200 grit silicon carbide paper, and ultra-sonically cleaned in ethanol prior to the tests. Isothermal corrosion tests were conducted in both S-CO$_2$ (200 bar) and atmospheric pressure CO$_2$ (1 bar) at 550, 600 and 650 ºC for 1000 h. After the corrosion tests, oxide layer and underlying matrix was characterized by X-ray diffractometer (XRD) and transmission electron microscope (TEM) with energy dispersive spectroscope (EDS) and selected area diffraction (SAD).

2.2 Effect of CO$_2$ Pressure on Corrosion Resistance

Fig. 1 shows the weight gain results of specimens corroded in S-CO$_2$ (200 bar) and CO$_2$ (1 bar) at 550, 600 and 650 ºC for 1000 h. As shown in the figure, weight gain are quite small for all test materials up to 650 ºC. For Ni-base alloys (Alloy 600 and Alloy 690), the weight gain in S-CO$_2$ is somewhat larger than that in CO$_2$ while the difference depending on CO$_2$ pressure is not significant for Alloy 800HT.
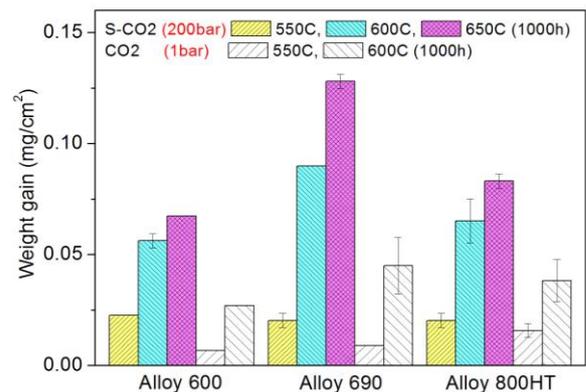
Fig. 1. Results of weight gain corroded in S-CO$_2$ (200 bar) and CO$_2$ (1 bar) at 550, 600 and 650 ºC for 1000 h.

Figs. 2 shows the thin film XRD results of the S-CO$_2$ and CO$_2$ corroded specimens at 600 ºC representatively. For both test conditions, the detected peaks in XRD analysis are identical, indicating similar oxide formation regardless the CO$_2$ pressure. In all test condition, the strongest peaks are from the matrix because of the thin oxide layer. Other than the matrix peaks, the major peaks are those of chromia (Cr$_2$O$_3$) in all test conditions and the peak intensities become stronger as temperature increases.

Table 1. Chemical compositions of chromia-forming austenitic alloys in this study (in wt.%)

	Ni	Cr	Fe	C	Mo	Mn	Ti	Al	Si	Cu	Etc.
Alloy 600	Bal.	16.1	9.3	0.08	-	0.3	0.20	0.16	0.3	0.02	-
Alloy 690	Bal.	28.4	8.3	0.02	-	0.2	0.26	0.3	0.2	0.01	-
Alloy 800HT	33.9	21.0	42.3	0.06	0.2	0.9	0.55	0.48	0.4	0.1	0.05 Co

In addition to chromia, the minor peaks of oxides such as $Mn_{1.5}C_{1.5}O_4$ and TiO_2 are formed depending on composition and test temperature. Therefore, the small weight gain in Fig. 1 could be explained with the formation of chromia layer in all test conditions. The same peaks of XRD analysis could be explained with similar oxygen partial pressure in between S-CO2 and atmospheric pressure CO2 [5].

(a)

(b)

(c)
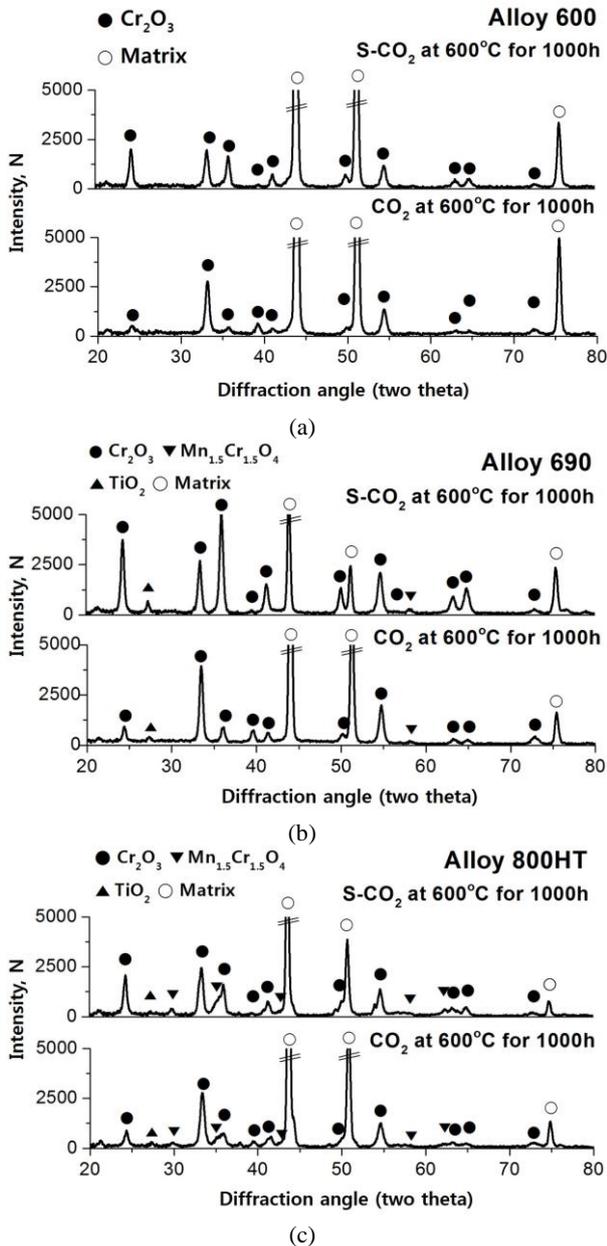
Fig 2. Results of XRD analysis corroded in S-CO2 and CO2 at 600 °C for 1000 h; (a) Alloy 600, (b) Alloy 690, and (c) Alloy 800HT.

2.3 Characterization of Oxide Layer and Underlying Matrix

Figs. 3 show the cross-sectional oxide layer and underlying matrix of 600 °C corroded specimen in S-CO2 environment. As shown in the figures, the oxide layer mostly consists of Cr as confirmed in XRD analysis. In addition, Small amount of Al and Ti are also detected at the interface between the chromia layer and underlying matrix, suggesting the existence of Al_2O_3 and TiO_2.

(a)

(b)

(c)
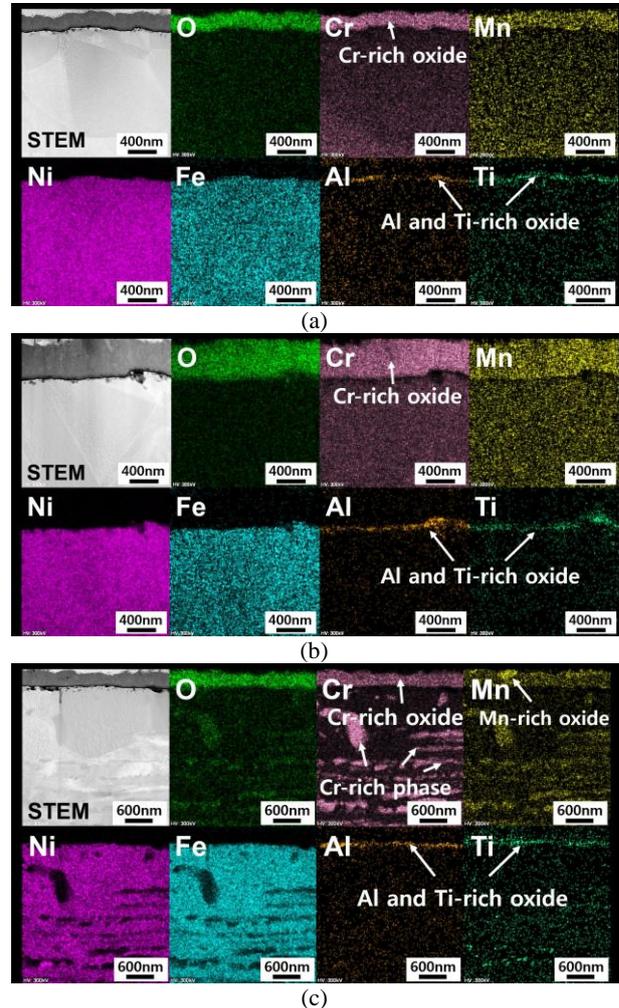
Fig. 3. Cross-sectional STEM micrograph and EDS mapping images of (a) Alloy 600, (b) Alloy 690, and (c) Alloy 800HT corroded in S-CO2 at 600 °C (200 bar) for 1000 h.

In the matrix below chromia layer, any precipitation are not observed in Ni-base alloys (Figs 3(a) and (b)) while a large amount of discrete particles (Cr-rich phase) are formed in Alloy 800HT (Fe-Ni-Cr alloy, Fig 3(c)) after S-CO2 exposure. Based on the SAD patterns analysis, these are identified as Cr-rich $M_{23}C_6$ carbides with FCC structure. Therefore, the carburization in S-CO2 environment is primarily affected by whether the matrix is Fe-rich or Ni-rich, but less by Cr content and the presence of Cr-rich oxide layer.

Besides, the cross-sectional TEM analysis of CO2 exposed specimens is in progress. The formation and degree of carburization of Alloy 800HT will be discussed depending on CO2 pressure.

3. Conclusions

Corrosion and carburization behaviors of three chromia-forming austenitic alloys (Ni-base alloys and Alloy 800HT) were evaluated in $S\text{-}CO_2$ (200 bar) and CO_2 (1 bar) environment at 550–650 ^oC for 1000 h. For all test materials, a good corrosion resistance was exhibited by the formation of thin chromia (Cr_2O_3) with small amount of minor oxides such as $Mn_{1.5}Cr_{1.5}O_4$, Al_2O_3, and TiO_2. For the Alloy 800HT corroded in $S\text{-}CO_2$, carburized region of Cr-rich $M_{23}C_6$ carbides was formed in the underlying matrix of chromia layer, but not in Ni-base alloys. It could indicate that the carburization in the matrix was primarily dependent on whether matrix is Fe-base or Ni-base despite of the presence of Cr-rich oxide layer.

Acknowledgements

REFERENCES

[1] Y.I. Chang, P.J. Finck, C. Grandy, Advanced burner test reactor preconceptual design report, Argonne National Laboratory report, ANL-ABR-1 (ANL-AFCI-173) 2006.
[2] G. Cao, V. Firouzdor, K. Sridharan, M. Anderson, T.R. Allen, Corrosion of austenitic alloys in high temperature supercritical carbon dioxide, Corrosion Science, Vol. 60, p. 246, 2012.
[3] V. Firouzdor, K. Sridharan, G. Cao, T.R. Allen, Corrosion of a stainless steel and nickel-based alloys in high temperature supercritical carbon dioxide environment, Corrosion Science, Vol. 69, p. 281, 2013.
[4] B.A. Pint, J.R. Keiser, The effect of temperature on the sCO2 compatibility of conventional structural alloys, Proceeding of the 4th international symposium-supercritical CO2 power cycles, Pittsburgh, Pennsylvania, Sep. 2014.
[5] P.A. Strakey, O.N. Dogan, G.R. Holcomb, G.A. Richards, Technology needs for fossil fuel supercritical CO2 power systems, Proceeding of the 4th international symposium-supercritical CO2 power cycles, Pittsburgh, Pennsylvania, Sep. 2014.